

ACCELERATION OF COMPACT TOROID PLASMA RINGS
FOR FUSION APPLICATIONS

C.W. Hartman, W.L. Barr, J.L. Eddleman, M. Gee,
J.H. Hammer, S.K. Ho, B.G. Logan, D.J. Meeker,
A.A. Mirin, W.M. Nevins, L.J. Perkins,
D.E. Shumaker, A. Leonard, P.B. Parks,
H. Mc Lean, E. Morse and D. R. Solvin

This Paper was Prepared for Submittal to
IAEA 12th International Conference on Plasma
Physics and Controlled Nuclear Fusion Research
Nice, France
October 12-19, 1988

August 26, 1988

The logo of the Lawrence Livermore National Laboratory is a large, stylized 'V' shape. The 'V' is composed of several horizontal layers of different shades of gray, creating a 3D effect. The text 'Lawrence Livermore National Laboratory' is written in a sans-serif font, following the curve of the right side of the 'V'.

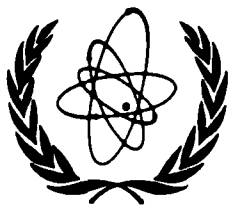
Lawrence
Livermore
National
Laboratory

This is a preprint of a paper intended for publication in a journal or proceedings. Since changes may be made before publication, this preprint is made available with the understanding that it will not be cited or reproduced without the permission of the author.

CIRCULATION COPY
SUBJECT TO RECALL
IN TWO WEEKS

DISCLAIMER

This document was prepared as an account of work sponsored by an agency of the United States Government. Neither the United States Government nor the University of California nor any of their employees, makes any warranty, express or implied, or assumes any legal liability or responsibility for the accuracy, completeness, or usefulness of any information, apparatus, product, or process disclosed, or represents that its use would not infringe privately owned rights. Reference herein to any specific commercial products, process, or service by trade name, trademark, manufacturer, or otherwise, does not necessarily constitute or imply its endorsement, recommendation, or favoring by the United States Government or the University of California. The views and opinions of authors expressed herein do not necessarily state or reflect those of the United States Government or the University of California, and shall not be used for advertising or product endorsement purposes.



INTERNATIONAL ATOMIC ENERGY AGENCY

**TWELFTH INTERNATIONAL CONFERENCE ON PLASMA PHYSICS
AND CONTROLLED NUCLEAR FUSION RESEARCH**

Nice, France, 12-19 October 1988

IAEA-CN-50/H-1-11

Acceleration of Compact Toroid Plasma Rings for Fusion Applications

C.W. HARTMAN, W.L. BARR, J.L. EDDLEMAN, M. GEE, J.H. HAMMER, S.K. HO, B.G. LOGAN, D.J. MEEKER, A.A. MIRIN, W.M. NEVINS, L.J. PERKINS and D.E. SHUMAKER

*Lawrence Livermore National Laboratory,
Livermore, CA 94550, USA*

A. LEONARD and P.B. PARKS

*General Atomic,
San Diego, CA 92138, USA*

H. MC LEAN, E. MORSE, and D.R. SOLVIN,

*University of California,
Berkeley, CA 94720, USA*

Acceleration of Compact Toroid Plasma Rings for Fusion Applications

Abstract

We describe experimental results for a new type of collective accelerator based on magnetically confined compact torus (CT) plasma rings and discuss applications to both inertial and magnetic fusion. We have demonstrated the principle of CT acceleration in the RACE device with acceleration of 0.5 mg ring masses to 400 km/s and 0.02 mg ring masses to 1400 km/s at $\geq 30\%$ efficiency. Very low mass rings have reached 2500 km/s. We have also observed ring focusing by ~ 3 -fold in radius. Scaling the CT accelerator to the multi-megajoule level could provide an efficient, economical driver for inertial fusion (ICF) or magnetically insulated inertial fusion. Efficient conversion to x-rays for driving hohlraum-type ICF targets has been modeled using a radiation-hydrodynamics code. At less demanding conditions than required for ICF, a CT accelerator can be applied to fueling and current drive in tokamaks. Fueling is accomplished by injecting CTs at the required rate to sustain the particle inventory and at a velocity sufficient to penetrate to the magnetic axis before CT dissolution. Current drive is a consequence of the magnetic helicity content of the CT, which is approximately conserved during reconnection of the CT fields with the tokamak. Major areas of uncertainty in CT fueling and current drive concern the mechanism by which CTs will stop in a tokamak plasma and the effects of the CT on energy confinement and magnetic stability. Bounds on the required CT injection velocity are obtained by considering drag due to emission of an Alfvén-wave wake and rapid reconnection and tilting on the internal Alfvén time scale of the CT. Preliminary results employing a 3-D, resistive MHD code show rapid tilting with the CT aligning its magnetic moment with the tokamak field. Requirements for an experimental test of CT injection and scenarios for fueling a reactor will also be discussed.

1. INTRODUCTION

In this paper we introduce the concept of the compact torus accelerator [1] and describe experimental results for the RACE (Ring ACcelerator Experiment) device [2]. Modeling of fusion applications is then discussed: first the use of highly focused, high-power density rings for inertial fusion and secondly the application of a compact-torus accelerator to fueling and current drive for tokamaks. We discuss requirements for an experimental test of tokamak fueling and the power requirements for fueling or current drive in a reactor.

2. ACCELERATOR CONCEPT

Magnetic confinement of plasma in the rings is the key feature of the accelerator concept. The plasma is confined by a nearly force-free, compact torus field structure consisting of a dipole-like poloidal field with an entrapped toroidal field, produced by currents flowing in the plasma and image currents in nearby conductors. A compact torus is shown schematically between the accelerator electrodes in Fig. 1. The ring field and confined plasma is magnetically accelerated in the coaxial electrode configuration shown in Fig. 1 with the ring acting as a moving armature as in a coaxial-rail gun. Shear

of the ring field provides a stability threshold against the Rayleigh-Taylor instability [3] as the ring is accelerated.

Stability of the confined plasma and field configuration, and long confinement time allows us to accelerate the ring over distances large compared to the characteristic ring dimensions and to a directed kinetic energy much greater than the internal magnetic and thermal energy of the ring. A directed kinetic energy ~ 10 times the internal magnetic energy of the compact torus has been reached in RACE. The internal magnetic energy of the ring is typically much greater than the thermal energy.

When a high ratio of kinetic to magnetic energy has been achieved, focusing to higher energy and power density is achieved by translating the rings into conical electrodes. The ring momentum carries the ring toward the apex of the cone, compressing the compact torus fields which are constrained to lie between the electrodes and focusing the confined plasma. Compression of ring magnetic fields increases the ring-magnetic energy at the expense of kinetic energy, and leads to reflection of the ring if the compression ratio is too large.

3. EXPERIMENTAL APPARATUS AND RESULTS

The plasma rings are produced by a magnetized coaxial plasma gun at the beginning of the accelerator shown in Fig. 1. The gun is 50 cm long with an outer/inner diameter of 35 cm/20 cm and has both inner and outer solenoids which can be energized by a 5 kV, 250 kJ electrolytic capacitor bank. Gas is fed into the gun with eight electromagnetically driven gas valves having a total plenum volume of 0.5 cc. The gas used is hydrogen (helium, argon, or mixtures thereof have also been examined). The gas is broken down and plasma and B_θ field are ejected from the gun by discharging a 60 kV, 200 kJ, low inductance capacitor bank between the inner and outer gun electrodes. As in similar magnetized gun experiments, [4-6] firing the gun results in emergence of a spheromak-type compact torus near the gun muzzle. In RACE, the ring is formed in the inter-electrode region at the beginning of the accelerator section (see Fig. 1). The straight coaxial accelerator electrodes were initially 6 meters long with an outer/inner diameter of 50 cm/20 cm, and are housed in a vacuum vessel 1.5 meters in diameter. Conically converging electrodes for ring focusing have been substituted for the final 2 meters of straight electrodes during the most recent operations as shown in Fig. 1. Rings are accelerated axially by $\vec{J} \times \vec{B}$ forces when the 260 kJ, 120 kV accelerator bank is discharged. The accelerating B_θ field is fed through an annular slot between the inner gun and inner accelerator electrodes as shown in Fig. 1.

The diagnostics consist of current and voltage monitors for the banks, visible light and VUV detectors, B-loop probes arrayed circumferentially (for symmetry) and axially (for trajectory), and Helium-Neon and CO₂ laser interferometers for measuring the line-integrated electron density.

The first experiments with all stainless-steel electrodes and H₂ gas injection demonstrated formation of compact torus rings suitable for acceleration having total magnetic energy of 5-10 kJ and ring lengths of 50-100 cm. Acceleration was observed to $v_{\text{ring}} \approx 4 \times 10^7$ cm/s with a ring mass of 5×10^{-4} gm and a kinetic energy of ≈ 40 kJ (out of 100 kJ of accelerator bank energy) inferred from trajectory analysis. The ring mass was not well correlated with the amount of injected gas and was somewhat high for matching the transit time of the ring to the quarter cycle time of the accelerator

bank. Subsequent experiments have been conducted with tantalum liners on the gun and accelerator electrodes, and glow discharge cleaning. Electrode contributions to the ring mass have been reduced, resulting in acceleration up to $v \approx 2.5 \times 10^8$ cm/s.

Proving the principle of ring acceleration has required demonstration of several significant features. The most fundamental of these is the observation of the integrity of the ring under acceleration. Figure 2 shows the time dependence of the axial magnetic field (B_z) observed by probes at the outer electrode as a ring moves down the accelerator. The ring B_z field at the electrode is typically 3-10 times the ring B_θ field (an ideal spheromak-type ring has $\vec{B} = B_z \hat{z}$ only at the outer electrode). The accelerating B_θ field is observed to rise sharply behind the ring. We have observed approximate preservation of the ring field profile and intensity for the entire 6 meters of the linear acceleration section, with some changes in response to acceleration such as steepening of the trailing edge as seen in Fig. 2.

From interferometer data, we observed that the plasma is well confined to the ring-magnetic fields. The mass of the ring (assuming it is constituted of hydrogen) is within about 30% of the mass estimated from the ring trajectory given the measured magnetic forces on the ring [2]. The current sheet position, calculated from the measured time-varying inductance of the accelerator also closely tracks the ring trajectory, indicating that the current and the associated accelerating force flows through the ring rather than intervening plasma. For the shot shown in Fig. 2, the ring reached a directed kinetic energy of 10 kJ out of the accelerator bank energy of 47 kJ.

We observe ring focusing with an array of magnetic probes distributed along the conical electrode. Several types of behavior are seen as rings impinge on the cone: reflection of the ring completely out of the cone after focusing by factors of 2-3 in radius; partial reflection followed by ring stagnation in the cone; ring stagnation without obvious reflection. The stagnated rings persist for $\simeq 100\mu\text{s}$. The cone converges to a small enough radius that the rings are generally reflected or stagnated before they can exit the cone. Field amplification is also observed by factors of order four, e.g., a 1 kG ring at the entry of the cone compressing to 4 kG at the reflection point of between 2 and 3 fold radial compression.

In summary, we have conducted experimental studies of compact torus formation, acceleration and focusing on the RACE device. The data supports the basic concept of a stable, well-confined plasma ring that undergoes acceleration and focusing in a manner consistent with simple models of momentum and energy balance.

4. INERTIAL FUSION DRIVER

Application of the compact torus accelerator to inertial fusion requires ring kinetic energy $\gtrsim 10$ MJ, with velocities $> 10^8$ cm/s and power densities in the range $10^{15} - 10^{16}$ watts/cm². Point model calculations of ring dynamics [7] suggest that attainment of these high-power densities can be achieved in an accelerator ~ 10 meters in length with a driving capacitor bank energy (or equivalent energy source) of 2-3 times the final ring kinetic energy. The accelerator would employ a conical "pre-compression" stage in addition to the final focusing stage which allows energy input on the $10\mu\text{s}$ time scale and hence modest bank voltages (< 500 kV) and cheap ($\sim 1\$/\text{Joule}$) energy storage.

In the regime where the ring kinetic energy dominates the magnetic energy and the gyro-radius of ions moving at the CT velocity and in the CT magnetic field is greater

than the CT linear dimension, it is expected that the plasma will act as an un-magnetized ion beam on impact with a target. In principle, polarization fields from the magnetized electrons could inhibit cross-field ion motion, however strong Rayleigh-Taylor instability [8] should preclude this possibility. In the CT parameter regime relevant to an ICF driver, 1-D calculations employing a radiation-hydrodynamics code show efficient conversion of the beam energy to x-rays for a hohlraum type ICF target. For a xenon CT with 5 MJ kinetic energy moving at a velocity 5×10^8 cm/s impacting on a thin foil, approximately 80% of the incident kinetic energy is converted to thermal x-rays. We have also found that conversion to x-rays can be efficient ($\sim 50\%$) in the limit that the magnetic field inhibits cross-field motion of the plasma. In this case the CT plasma is heated by a shock wave when the ring strikes the target. The thermal energy is converted efficiently to plasma bremsstrahlung and line radiation for sufficiently high CT ion density (e.g., $n_{xe} > 10^{18}/\text{cc}$).

Also, the imbedded magnetic field of the compact torus makes the accelerator a natural candidate for driving magnetically insulated inertial fusion (MICF) targets [9]. In this scheme, the fusion-fuel is not compressed, remaining below solid density, and is confined by a high-density tamper. The magnetic field imbedded in the fuel (in this case, the CT field) suppresses cross field transport of heat and alpha particles.

5. TOKAMAK FUELING BY COMPACT TORUS INJECTION

Recently there has been growing interest in alternative methods of fueling tokamak reactors because it appears unlikely that a pellet fueling system will be capable of depositing fuel near the magnetic axis. A CT injected with $\rho_{CT} V_{CT}^2 > B_{tokamak}^2/4\pi$ is expected to propagate across the tokamak magnetic field [10,11] as shown in Fig. 3. The initial velocity, radius and density of the CT will be chosen so that the CT stops and reconnects with the tokamak field near the magnetic axis. This would allow deep penetration fueling in a reactor grade plasma and attainment of the peaked density profiles that allow ignition in machines that have only marginal energy confinement times.

5.1. Compact Torus Dynamics

Since that CT plasma is a good conductor on the time scale involved (a few μsec), it will tend to develop screening currents that exclude the tokamak field from the CT. To the extent that the CT behaves as a perfect conductor, the dominant drag would be caused by excitation of Alfvén waves in the tokamak plasma and the CT dynamics would be determined by this drag force together with the ∇B^2 force. If the CT does not behave as a perfect conductor, but can undergo magnetic reconnection, the screening currents will dissipate and the CT dipole-moment will interact strongly with the tokamak field and cause tilting as shown in Fig. 3. The dynamics of the CT are thus critically dependent on the rate at which magnetic-field-line reconnection can occur, which is a subject of some controversy. From models developed in an astrophysical context [12], we can examine the rapid reconnection limit $\tau \cong \tau_A$ (Petschek) and the slow limit $\tau \cong \sqrt{\tau_A \tau_R}$ (Sweet-Parker) where τ = reconnection time, $\tau_A = r/V_A$ = Alfvén time, $\tau_R = \frac{\eta r^2}{\mu_0}$ = resistive time, r = CT radius, $V_A = \sqrt{B/4\pi\rho_{CT}}$, η = CT resistivity. For rapid reconnection, if the CT is to penetrate the tokamak minor radius, a , before reconnection and tilting, then the

Table I: Suggested parameters for CT injection fueling of the engineering test reactor.

	Fast reconnection	Slow reconnection
Injection velocity (km/sec)	750	460
DT mass/shot (mg)	4.8	0.037
Rep-rate (Hz)	0.93	122
Energy/shot (J)	1.35×10^6	1.95×10^4
Average wall-plug power (MW)	~ 2.5	~ 2.4
Initial CT diameter at entrance port (m)	0.5	0.067

required kinetic energy density is [11]

$$\tau \cong \tau_A = a/V_{CT} \rightarrow \rho_{CT} V_{CT}^2 \cong \frac{B^2}{4\pi} \left(\frac{a}{r}\right)^2 \quad (1)$$

For slow reconnection, Alfvén drag is usually the dominant irreversible process. The drag power is given by [10] $P_{DRAG} \cong 2\pi r^2 \rho_o V_{CT}^2 V_{AO}$ where the subscript “o” refers to the tokamak parameters. The required kinetic energy density is then

$$\rho_{CT} V_{CT}^2 \cong \frac{B^2}{4\pi} \left(\frac{a}{r}\right)^2 \frac{\rho_o}{\rho_{CT}} \quad (2)$$

Since $\rho_o/\rho_{CT} \ll 1$ for a CT fueling scheme, the required energy density is much less if the slow reconnection model applies. Other constraints are:

$$\frac{N_{CT}}{N_{tokamak}} \ll 1, \quad \frac{a}{V_{CT}} < \tau_R, \quad \beta_{CT} \gtrsim 0.2, \quad f_{inject} \gtrsim 10^3 \text{ Hz}, \quad \frac{r}{a} \ll 1 \quad (3)$$

where N_{CT} , $N_{tokamak}$ are the particle inventories and f_{inject} is the injection frequency. In the slow reconnection limit, the radially outward force due to gradients in magnetic pressure can be important, $F_{\nabla B^2} = \frac{1}{3} \frac{B^2 r^3}{R}$ (R is the tokamak major radius). Reconnection must be fast enough to disassemble the CT before it is expelled by $F_{\nabla B^2}$. Combining constraints (3) with Eqs. (1) or (2) for the fast or slow reconnection limits results in typical fueling systems as shown in Table 5.1 for the ETR type tokamak reactor [11].

5.2. MHD Simulation of Compact Torus Reconnection in the Tokamak Field

The interaction of the CT with the tokamak is studied using the non-linear, compressible, resistive MHD code TEMCO [13]. Rather than treat this very complicated problem in its fullest, we assume that the compact toroid is initially placed at rest in a uniform magnetic field modified to exclude the spherical CT with a density 10 times that of the surrounding tokamak. The symmetry axis of the CT is initially at right angles to the external field direction. The simulation shows that the CT tilts 90 degrees in about an Alfvén time, as shown in Fig. 4, its magnetic moment lining up with the tokamak magnetic field. The subsequent magnetic evolution shows rapid dissolution of the CT field structure. The results are preliminary in that further studies are needed to give confidence that the modeling of the transition region between the CT and tokamak fields is accurate.

5.3. Experimental Test of CT Injection

Experimental tests of CT injection are being proposed [14] for the TEXT and MTX tokamaks to obtain data concerning these critical issues. Small CTs ~ 4 cm diameter with kinetic and magnetic energy $\simeq 5$ KJ, and plasma inventories of $\simeq 10\%$ of the tokamak plasma inventory would be produced by a magnetized coaxial plasma gun.

For simplicity the first tests would be performed without an accelerator stage but with the plasma gun alone. CTs emerge from a plasma gun with kinetic energy \sim the magnetic energy ($\rho_{CT} V_{CT}^2 \simeq B^2/4\pi$) so, if the tilt constraint is operable as discussed in Sec. 5.1, the CT may not penetrate to the magnetic axis. Penetration to the axis should be possible if the slow reconnection model applies, although partial penetration would still provide valuable information about the CT dynamics. An experimental test will provide data on other important issues: gun-produced plasma purity, gas efficiency, gun erosion, possible degradation of tokamak energy confinement or excitation of MHD instabilities of the tokamak.

6. TOKAMAK CURRENT DRIVE BY CT INJECTION

In addition to particles, the CT also carries magnetic helicity. It is expected that the magnetic helicity will be conserved during the reconnection, hence the tokamak helicity and circulating current will be increased with each injected CT, giving a net current drive. The helicity content of a tokamak is given approximately by

$$k \approx \Psi_P \Phi_T$$

where Ψ_P , Φ_T are the tokamak poloidal, toroidal flux. It follows from the conservation of helicity that when a CT is injected and the initial tokamak current profile has been restored; then the plasma current must increase by an amount

$$\delta I_P \approx \frac{2\delta k}{\mu_o R \Phi_r} \approx \frac{2r_{CT} W_m}{\pi R \Phi_r}, \quad (4)$$

where W_m is the magnetic energy of the CT, and we have used the fact that the helicity content of the CT is $\delta k \approx r_{CT} W_m$.

The condition that we drive all of the current is that all of the helicity in the tokamak be replaced in an L/R time,

$$\frac{\delta I_P}{I_P} = \frac{\tau_{CT}}{\tau_{L/R}}. \quad (5)$$

where $\tau_{L/R}$ is the L/R time including only the inductance of the plasma column and τ_{CT} is the time between CT's.

From Eqs. (4) and (5) the power required for the CT current drive system is given by

$$P_{CT} \approx \frac{\pi R \Phi_T I_P}{2r \tau_{L/R}} \left(1 + \frac{4\pi \rho_{CT} V_{CT}^2}{B_0^2} \right) \quad (6)$$

Using the tilt constraint, Eq. (1) in Eq. (6) and typical tokamak reactor parameters leads to $Q \simeq \frac{P_{fusion}}{P_{CT}} \simeq 50$. for CT current drive.

ACKNOWLEDGMENTS

This work was performed under the auspices of the U.S. Department of Energy by Lawrence Livermore National Laboratory under Contract W-7405-Eng-48.

References

- [1] HARTMAN, C.W. and HAMMER, J.H., *Phys. Rev. Letter* **48** (1982) 929.
- [2] HAMMER, J.H., HARTMAN, C.W., EDDLEMAN, J.L. and McLEAN, H.S., "Experimental Demonstration of Acceleration and Focusing of Magnetically Confined Plasma Rings", Lawrence Livermore National Laboratory Report, June 22, 1988, Submitted to Physical Review Letters.
- [3] MIKHAILOVSKII, A.B., Theory of Plasma Instabilities, Vol. 2: Instabilities of an Inhomogeneous Plasma (Consultants Bureau, New York, 1974), p. 177.
- [4] TURNER, W.C., et.al., *Phys. Fluids* **26**, (1983) 1965.
- [5] BARNES, C.W., et.al., *Phys. Fluids* **29**, (1986) 3415.
- [6] UYAMA, T., et. al., *Nucl. Fus.* **27**, (1987) 799.
- [7] HARTMAN, C.W., EDDLEMAN, J.L., HAMMER, J.H., MEEKER, D.L. in Proceedings of the 4th International Conference on Emerging Nuclear Systems, Madrid, Spain, 1986 (World Scientific, Singapore, 1986) p. 158.
- [8] HUBA, J.D., and LYON, J.G., *Phys. Rev. Lett.* **59**, (1987) 2971.
- [9] HASEGAWA, A., et. al., *Nucl. Fus.* **28** (1988) 369.
- [10] PARKS, P.B., "Refueling Tokamaks by Injection of Compact Toroids," GA Report GA-A18933, December 1987. Submitted to Physical Review Letters.
- [11] PERKINS, L.J., HO, S.K. and HAMMER, J.H., "Deep Penetration Fueling of Reactor Grade Plasmas with Accelerated Compact Toroids," Lawrence Livermore National Laboratory, Livermore, CA, UCRL-96894, June 23, 1987, submitted to Nuclear Fusion.
- [12] VASYLIUNAS, V.M., *Rev. of Geophys. and Space Phys.*, **13** (1975) 303.
- [13] SGRO, A.G., MIRIN, A.A. and MARKLIN, G., *Phys. Fluids*, **30** (1987) 3219.
- [14] BARR, W.L. et. al., "Advanced Fueling Schemes for ITER: A Proposal to Investigate the Feasibility of Deep Penetration Fueling by Gun-Produced Compact-Toroid Plasmoids", Lawrence Livermore National Laboratory Report, LLL-PROP-00210, May 5, 1988.

Figures

Fig. 1. The RACE compact torus accelerator consisting of a coaxial plasma gun, a straight acceleration section and a focusing cone.

Fig. 2. Axial magnetic field at the RACE outer electrode ($r = 25$ cm) for different axial locations vs. time.

Fig. 3. Schematic of compact-toroid (CT) acceleration and interaction with the external tokamak toroidal field. As it traverses the external field, the CT rotates through a 90° angle due to the torque on its internal magnetic moment. Alignment of the CT poloidal field with the external field results in field-line reconnection and fuel deposition.

Fig. 4. Contours of the component of \vec{B} normal to the plotting surface ("toroidal" field) in resistive MHD simulations of a CT tilting in a tokamak field.

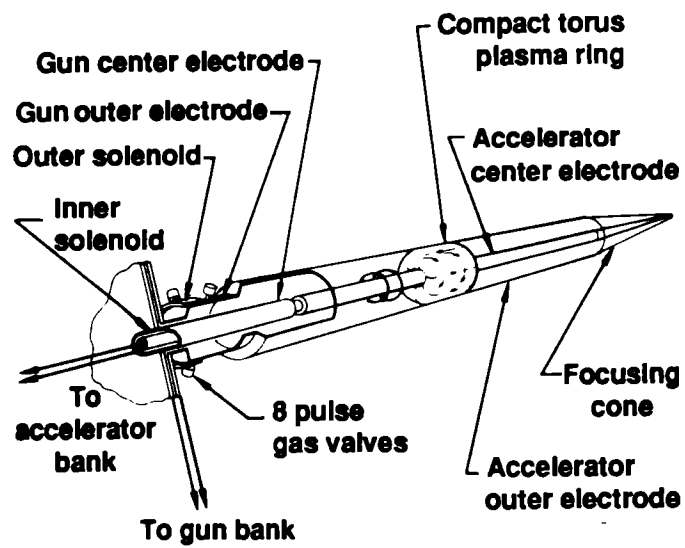


Figure 1

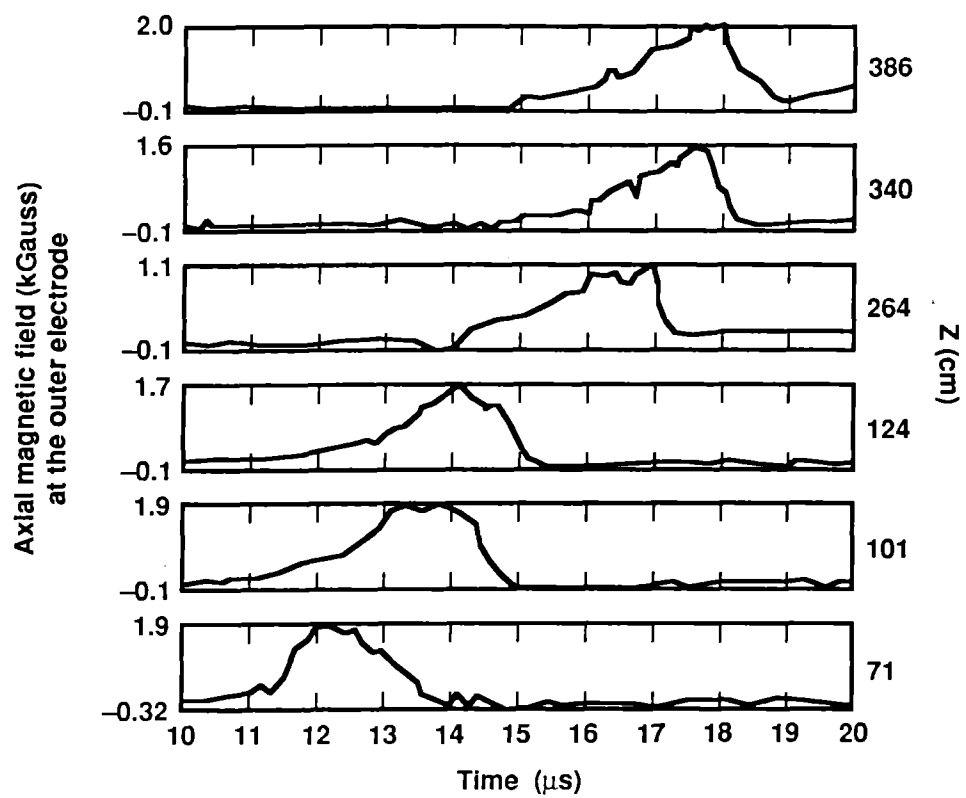


Figure 2

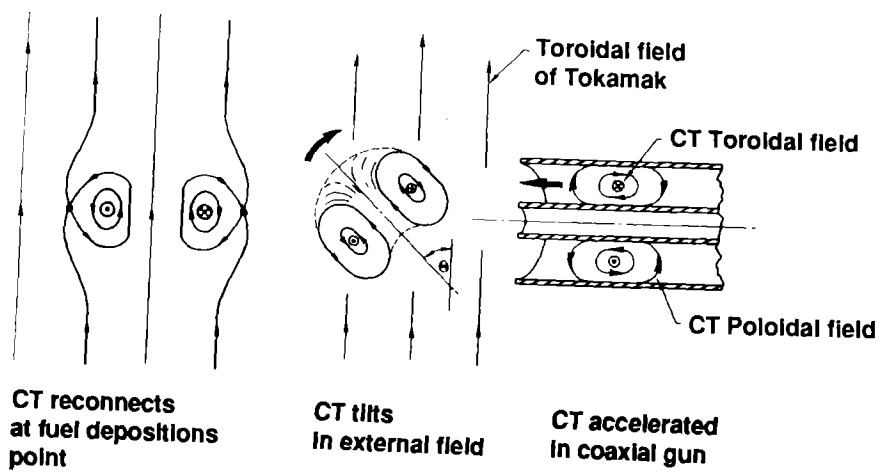


Figure 3

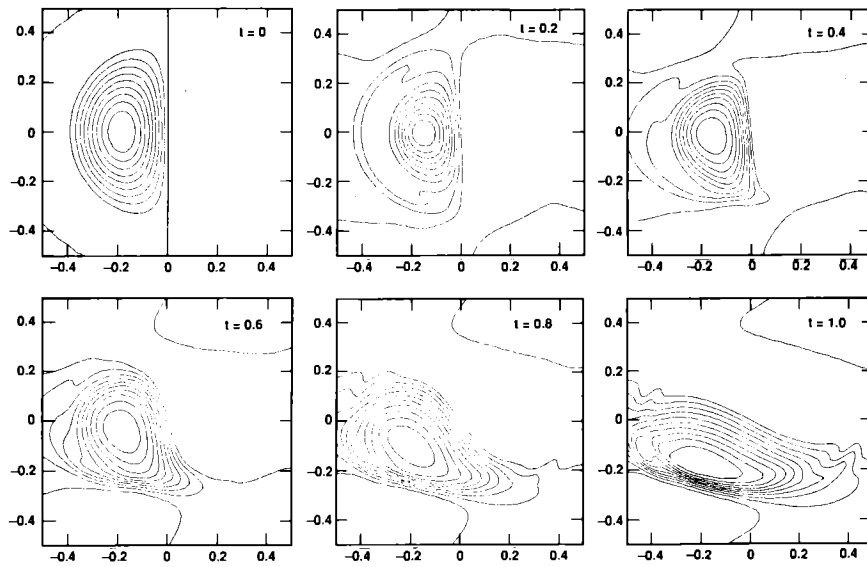


Figure 4

